

Chapter 5

Polymer Gradient Surfaces for Biomedical Applications

Paul M. Reynolds and Nikolaj Gadegaard

5.1 Introduction

5.1.1 Background

Biological systems interact with artificial polymeric materials in a complex, multi-stage, and iterative process of sensing and response [1]. The biological response at the cellular level to polymeric substrates has been studied at great length. However, this is often done on individual samples with a homogeneous feature. This results in experiments which are limited only to samples that the investigator can imagine — leaving potentially interesting samples or sample combinations hidden from use. Subtle variations in surface properties can have a drastic impact on cell response, and therefore a considered and careful approach must be employed in surface design and fabrication. Following the example set by combinatorial chemistry and high-throughput screening (HTS) applied to drug discovery by the pharmaceutical industry in the 1990s, [2] researchers are increasingly turning to similar methodologies in biomaterial design [3–10]. This involves creating high content samples for exploring the full sample space, usually taking the form of a highly multiplexed array platform, or a continuous variation of a single material property as a gradient. Creating such dense sample formats presents a series of unique challenges in both their fabrication and implementation. In the case of surface modification for biomedical applications, platforms must be created which offer broad variations in surface properties, and they must also be designed in such a way as to allow meaningful interpretation of often complex responses.

Gradients seem to offer the ideal solution in terms of manufacture and sample variation. Gradients may be fabricated in 2D or 3D, however whilst 3D studies are generally considered to be more representative of the in vivo architecture of most

N. Gadegaard (✉) · P. M. Reynolds
Division of Biomedical Engineering, School of Engineering,
University of Glasgow, Glasgow, UK
e-mail: Nikolaj.Gadegaard@glasgow.ac.uk

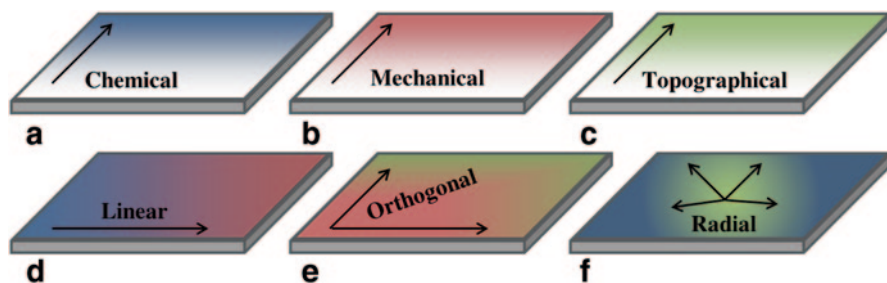


Fig. 5.1 Cells sense their environment through three main ‘columns’ of sensing: chemical, mechanical, and topographical. **a** Chemical gradients range from a simple change in surface energy, to surface modification with proteins, functional molecules, or peptides. **b** Mechanical gradients are a modulation of a mechanical property such as the Young’s modulus of a substrate. **c** Topographical gradients present a variation of surface structure, which have been shown to be a powerful manipulator of biological response. **d, e, f** These gradients of surface properties can be combined into linear **d** orthogonal **e** or radial gradients **f** which elicit the interplay between two material factors in a biological response

biological systems, they present problems in terms of fabrication, data acquisition, and data analysis. For this reason, studies investigating cellular response to engineered surface cues are predominantly carried out in 2D *in vitro* systems. The use of semiconductor fabrication techniques, which have consistently increased in resolution since their inception [11] has allowed 2D surface patterning at length scales which now approach that of single molecules, and surpassed that of the single cell many years ago [12]. Chemical, mechanical, and topographical features of a polymeric surface have all been shown to be capable of independently affecting cell behaviour and response to an engineered surface [1]. Gradients of each surface property can be fabricated independently or orthogonally to one another to create multiplexed parameter variations on a single substrate, Fig. 5.1.

Ease of fabrication, data analysis, and interpretation makes the use of linear gradients most favourable. Single properties may be varied in a single direction, Fig. 5.1a–c, or multiple may be varied in opposite directions to create a bidirectional linear gradient, Fig. 5.1d. Orthogonal variation of two parameters serves to create as many possible combinations of two surface parameters as possible. Radial gradients have surface properties which change continuously from a central point outwards, and are most often used when fabrication makes use of diffusion-based processes from a single point source [4, 13]. These gradients are least favourable due to the difficulties associated with mapping cell response to corresponding surface properties.

5.1.2 Gradient and Array Platforms

The distinction between gradient and array formats as HTS methods is an important one. A gradient is a continuous variation of a feature, such as structural dimension

or surface chemistry. This feature changes ‘continuously’ from one value to another, however its resolution is essentially defined by its nature—a gradient of chemistry may only change spatially in so much as its molecular structure allows. Arrays, however, are discrete variations in a surface parameter, separated or congruent on a single sample. These areas may be completely isolated from one another, or may exist on a single substrate and used in an open environment. Essentially, then, based on the property in question, an array might have a fine enough resolution so as to offer a working resolution which is comparable with a continuous gradient. (Fig. 5.2)

The key difference in understanding their use and implementation is that cells or molecules are free to move along or adsorb across a gradient platform, with cell motility yielding further information about how they interact with the surface. In an array platform, this is not possible—as cells or biomolecules interact with sample conditions which are isolated from each other, or at least separated spatially. There are benefits to each of these methods, and the impact of gradient or array formats should be carefully considered. Whether a continuous gradient or a microarray platform should be used must be taken into consideration, with Hook et al. suggesting that gradients are most useful in optimisation of surface properties, whereas microarray platforms are preferable in the discovery of new cell-material interactions[5]. Nonetheless, gradients represent a significant improvement on discrete material tests for screening the relative change in properties such as adsorption of nanoparticles or proteins, and cell behaviour itself.

The continuous nature of gradients can present a problem in experimental design, in that artefacts such as cell migration along the gradient and cell–cell communication across it are a unique part of the biological response. Instead some groups choose to prioritise the use of microarray platforms as these provide distinct variations in material properties and therefore produce data which is easier to interpret. These difficulties are offset by advantages such as a lower cell number and culture media usage—reduced biological variation between conditions and reduced sample material usage—these are significant advantages when working with rare or problematic biological specimens/materials.

5.1.3 *Cell-Surface Interactions*

Polymer surfaces can broadly be divided into three groups, based on their apparent mode of action, Fig. 5.1. They may provide topographical cues via their micro- and nanoscale architecture. Surfaces may also provide chemical cues which may comprise biomolecules directly tethered to the surface, or a tuned wettability which modulates protein adsorption. Finally, their mechanical properties such as stiffness and rigidity can direct biological activity. Here, we will present a series of emerging fabrication techniques which allow the creation of high content gradient platforms for all three classifications, including combinations of the three.

Preparing and characterising individual samples with different properties is a time consuming and costly approach to finding polymer materials which are fit for purpose. Including multiple conditions on a single sample, in the form of either

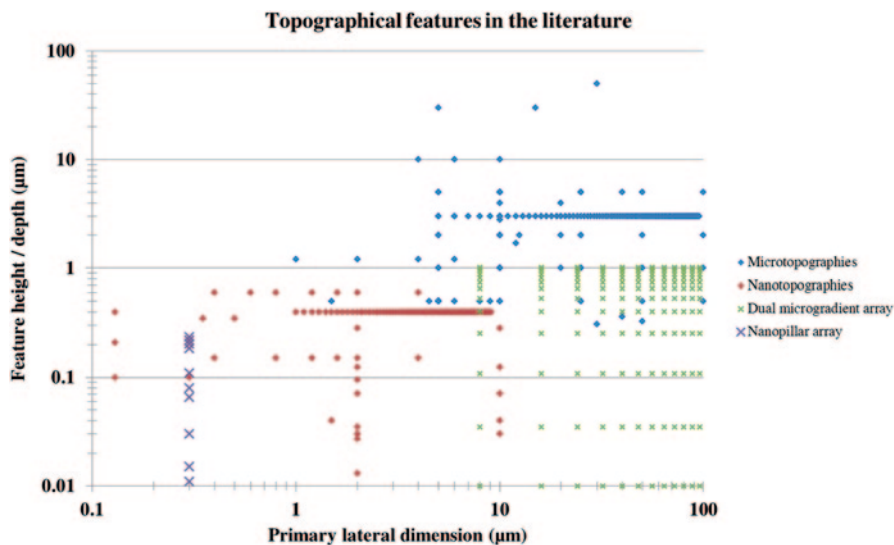


Fig. 5.2 a Graphical understanding of the literature. Collated data from 25 papers with at least 50 citations which use structured polymer microtopographies [14–24] or nanotopographies [25–38] to drive cellular response. We have chosen to focus only on structures produced by common semiconductor fabrication techniques, so as to simplify data comparison—as each study was conducted with certain feature dimensions in terms of feature height and lateral dimensions. Commonly, each paper is represented by one or two single points due to the limitations of fabricating individual, homogeneous samples. Alongside these datapoints, we have included work from our lab (nanopillar array [39] and dual microgradient array [40]) which seeks to more fully explore the sample space by using gradients of topographical features. Continuous variation of nanopillar height was used to investigate the differential response of fibroblast and endothelial cells to the surface, *blue* [39]. Furthermore, we have demonstrated the use of dual topographical gradients—variation of microgroove depth, with orthogonally varied microgroove pitch, *green* [40]. This demonstrates the ability of gradient platforms to more fully cover the sample space, rather than limiting results to a small subset of individually fabricated samples

arrays or continuous gradients, can greatly expedite the characterisation of biological response to it. High-content libraries of topographical motifs have been demonstrated as powerful tools for the discovery of optimal surface topographies, with a single 2×2 cm chip containing 2176 distinct geometric patterns generated algorithmically by combining three primitive shapes, fabricated by photolithography, and applied to the analysis of human mesenchymal stromal cells to these geometric combinations [41]. Simon and Gibson compiled an excellent review on combinatorial approaches to biomaterial design including both array and gradient formats [3]. Numerous other review articles are available for further reading [4–10]. Genzer et al. present a compilation of 24 innovative gradient fabrication methodologies, covering a broad range of functionalization methods for both polymeric and inorganic substrates. [4] Inorganic substrates such as silicon are often used as a substrate, which is functionalized with bioactive molecules. Whilst incompatible with direct applications in biological systems, the use of such substrates enables

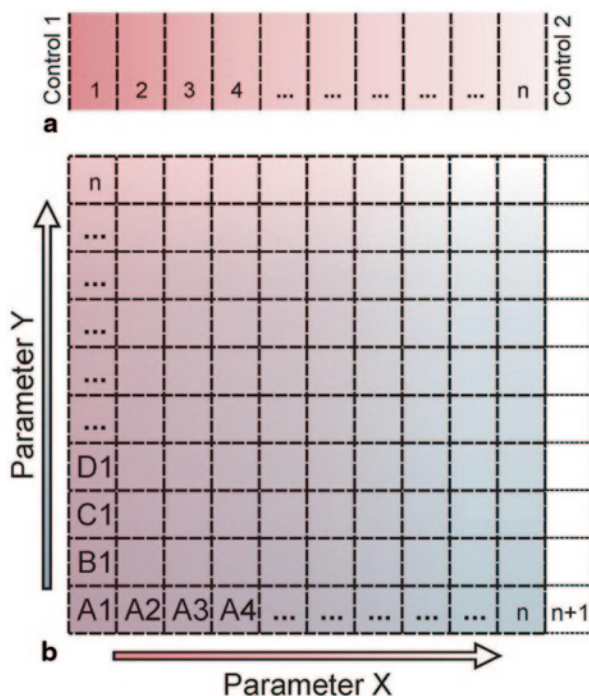


Fig. 5.3 Continuously varied surface parameters must be discretised for analysis. Cell culture studies have a theoretical maximum resolution of the spread of a single cell along the gradient axis. Whilst modern scanning stage microscopes and automated image analysis software makes this possible, the most common approach in the literature is to divide linear or 2D gradients into subunits of size L/n , where L is the total gradient length and n is the number of subunits. This yields an inherent variation in a single subunit, which is often presented as a uniform value in the literature, masking underlying variation in surface properties and therefore cell response. A square imaging array, captured with a camera which has a rectangular field of view will also be disproportionately loaded in each datapoint with variation in one axis versus the other. Both linear gradients, **a**, and multidimensional gradients, **b**, must be divided into subunits for image analysis

the screening of biological response to a variation in functionalization, which may then be translated onto compatible bulk materials [42]. In fact, the use of thin film polymer coatings alleviates the need for bulk materials to be fully compatible with prospective applications.

Besides discussing the three cues listed above, we will also address how such gradient substrates are evaluated. Commonly, they are simply discretised and analysed in a similar fashion to arrayed samples or platforms. In this respect, the use of gradients may seem counterproductive, if high resolution variations in surface parameters are simply reduced to single instance of a parameter, Fig. 5.3. The strength of parameter gradients lies in the fact that a spatially discretised gradient may include surface parameters which may not have been included in a spatially discretised array. In addition, fabrication of a wide range of surface parameters in a single process may be faster and more reliable than fabrication of individual samples.

Despite increasing resolution of surface characterisation techniques allowing a finer determination of the variation of a given property along a gradient, the literature does little to address the methodologies used to segment biological results on gradients. The default spatial unit of measurement is frequently found to simply be the width of an image frame, for example images captured at $\times 10$ magnification are commonly 800–1000 μm in width. These images become individual datapoints, when in reality they contain an intrinsic variation across them, depending on the spatial rate of change of the underlying gradient. This results in a quantisation of the gradient in a semi-arbitrary fashion, and is particularly inflexible to tolerances in the imaging method. For example, using a motorised stage to capture congruent images across a linear or 2D gradient relies strongly on accurately aligning the substrate and ensuring uniformity in imaging locations across samples.

The location of controls in investigations making use of gradient surfaces also merits some consideration. A surface gradient may occupy a given sample space, with blank control regions surrounding it. Our work on gradients of nanopillar height has shown differences in cell phenotype on flat regions which are adjacent to tall nanopillars versus short nanopillars [39]. Local migratory behaviours and cell–cell interactions influence cell response at these adjacent regions, as can be seen in Fig. 5.10 as an increase in cell number adjacent to one end of the linear gradient. Such effects, most prominent when comparing flat regions to a section of the gradient, must be considered as also having an influence on the patterned regions themselves. This can lead to situations whereupon scale up of a region of the gradient, after identifying it as driving a positive cellular response, a homogeneous sample covered in the same pattern does not elicit the same response. This inherent tendency for cross talk between cells on gradient platforms must be considered when interpreting results. Expansion of individual gradient points into larger homogeneous areas may not produce the same biological response, perhaps indicating that the complex gradient environment has a strong effect on the experiment.

5.1.4 Gradient Fabrication

In most cases, uniformity and homogeneity represent the gold standard in sample fabrication for biomedical engineering studies. Variability between experimental materials is recognised as a source of irreproducible results, slowing and distorting studies of cell-material interactions. As a result, there has been a vast deal of effort invested in ensuring that sample fabrication schemes are consistent and reproducible. This has meant that until relatively recently, there was little work available on the controlled fabrication of *nonuniform* gradient substrates. There has, however, been a recent increase in the reporting of new methods for the fabrication of gradient surfaces—encompassing chemical, topographical, and mechanical modifications of a range of materials [5, 43, 44]. Such samples are viable alternative to groups of individual samples as they can provide a more complete variation in a property, such as hydrophobicity. Conducting a full experiment on a single sample also reduces problems associated with biological variability between large numbers of samples. (Fig. 5.4)

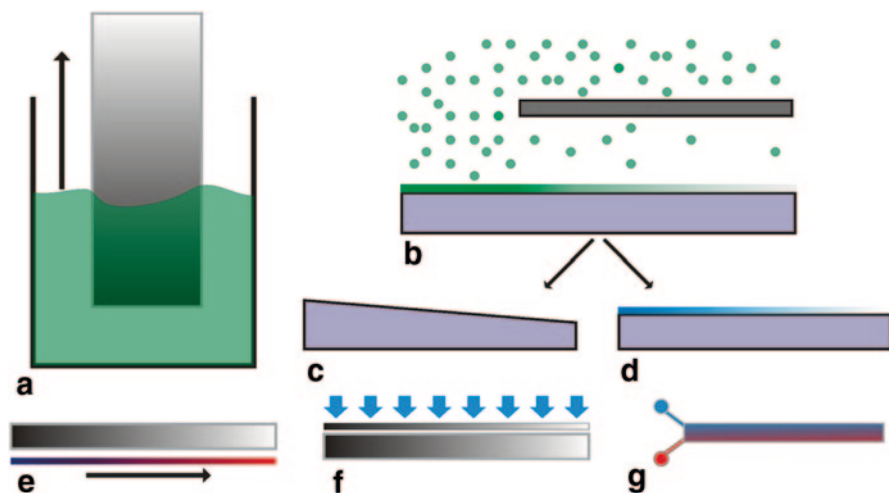


Fig. 5.4 Polymer gradient fabrication techniques. **a** Sample immersion and removal from a solution of monomer, solvent, or etchant—creating a gradient based on retraction rate. **b** Plasma polymerisation excited by RF glow discharge under a diffusion mask, yielding a decrease in monomer concentration into the channel which translates into a variation in deposited film thickness or chemical composition. Plasma polymer gradients may be used in their deposited state, **b**, as wettability gradients [45, 46], or they may be used as sacrificial masks in a dry etching process to transfer a gradient of etch depth into a substrate. **c** [39, 40] Monomers with reactive groups such as carboxyl [47] or amine groups may be functionalised after deposition with biomolecules such as proteins or short chain peptides [48]. **d**. **e** Polymer microspheres annealed on a temperature gradient have a continuously varying crystallinity across the sample [49–51]. **f** Greyscale lithography or localised UV irradiation can be used to deliver a gradient of light across a photoactive substrate [42, 52]. **g** Microfluidic mixing devices allow precise mixing of monomer solutions or suspensions of biomolecules into gradients on a surface [53–57].

Polymer gradients may be classified in terms of properties such as their mode of interaction with a biological system, their dimensionality, and their range (either steep or shallow). An overview of fabrication methods are presented below in Table 5.1.

5.2 Chemical Gradients

Chemical modification or tuning of a surface may take two forms; either guiding the way in which proteins and biomolecules interact and adsorb on the surface, or directly tethering biomolecules to the surface so as to present an artificially engineered interface. Ultimately, both methods affect cell response by the same means, whereby interrogation of the surface properties by a cell is changed. Density, type, and structure of adsorbed proteins have all been shown to influence cell behaviour and can be prepared by various methods. Plasma treatment of polymer surfaces—either the modification of a bulk polymer surface, or deposition of a polymer film,

Table 5.1 An overview of fabrication methods for gradients of surface chemistry, topography, and mechanical properties

	Fabrication method	Gradient type	Length scale	Speed	Ref
Chemical	Plasma polymerisation under a diffusion mask	Wettability/surface functionalization	Up to 20 mm	Moderate	[47, 58–61]
	Microfluidic mixing of component solutions	Surface functionalization	10 μ m to 1 mm	Slow	[53–57]
	Substrate movement through a vessel	Wettability/surface functionalisation	Up to 10 mm	Fast	[62–64]
Topographical	Direct write lithography	Micro or nano	Up to 10 mm	Slow	[18]
	Grey scale lithography	Micropatterning	Up to 10 mm	Fast	[42, 52]
	Annealing on a temperature gradient	Surface roughness/feature depth	Up to 10 mm	Moderate	[50, 65]
	Plasma polymer thickness gradient, used as sacrificial etch masks	Feature depth	Up to 10 mm	Moderate	[39, 40]
Mechanical	Curing under UV or thermal gradients, multilayer lithography	Elastic modulus	Up to 10 mm	Moderate	[66, 67]
	Microfluidic mixing	Elastic modulus	10 μ m to 1 mm	Slow	[53]

has been used extensively to tune the biological response of a surface. Cell adhesion to polymer surfaces may be enhanced or inhibited by glow discharge treatment through tuning of the water contact angle (WCA)—with a WCA of 70° appearing to be the optimal value for cell adhesion. Beyond modification of the surface energy many methods have been reported to create continuous variations in chemistry on a surface, with varying levels of complexity. As most existing chemical modifications are done in a homogeneous manner across a surface, adapting these methods to spatially vary the chemical modification is essential. This can be done by physically moving the sample through a solution [62–64], intricate mixing of reagents on a sample using microfluidics [53–57], annealing or curing a surface coating on a temperature gradient [51, 65], or plasma polymer deposition using either knife edge electrodes or through a series of apertures [68].

5.2.1 Wettability Gradients

Deposition of plasma polymer films through a diffusion mask can be used to tune the density of functional groups on a surface or to vary the hydrophobicity of a surface [46, 48, 59, 69]. By limiting the concentration of the monomer across the sample by covering the area, deposition rates can be varied along the diffusion mask. These films yield a conformal, pinhole free coating which can then be processed to covalently link biomolecules to its surface. Alternatively, the surface may be physically masked with a barrier held in close proximity, which is then gradually moved away, yielding a variation of plasma exposure time. Whilst this method has a more involved setup due to the requirement of building a mechanically actuated barrier inside a radio frequency discharge chamber, it is more flexible than deposition by diffusion gradient, as the rate and manner of movement can be tailored to produce various gradients. Such a mechanical barrier can readily be constructed from e.g. LEGO parts [70;Fig. 5.5].

Plasma polymer films are especially attractive due to the variety and scope for uses after the initial outlay on construction of the necessary processing equipment. Reaction chambers themselves are fairly simple to construct, generally consisting of a vacuum chamber, some means of exciting a plasma, for example copper band electrodes or parallel plate electrodes along with a radio frequency generator, and a monomer inlet with flow control [71–73]. Various monomers are available for deposition by plasma polymerisation, including hexane, acrylic acid, and allylamine among others [74–78]. Deposition of these polymers creates thin film coatings with unique properties for biomedical applications. Plasma polymerisation techniques are particularly amenable to the creation of gradients, with the use of a simple diffusion mask as shown in Fig. 5.6.

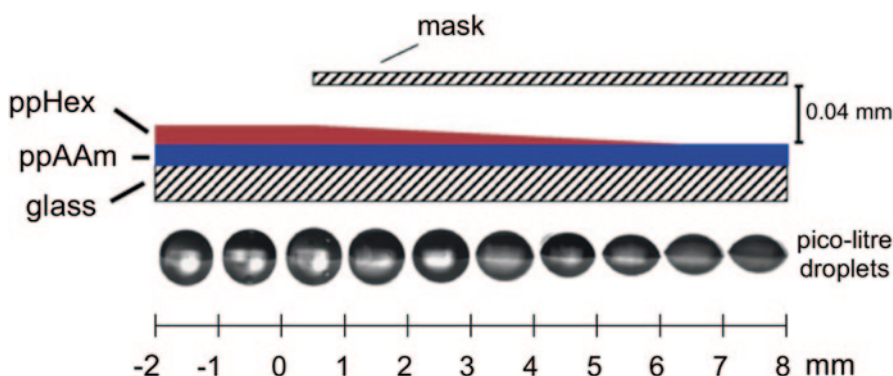


Fig. 5.5 Schematic of the experimental setup used to prepare a shallow diffusion gradient. The hexane plasma diffuses under the mask from the left-hand side onto a plasma polymerised allylamine coated glass slide while all the other edges are sealed. Representative images of the water contact angle (WCA) droplets used for the WCA analysis are inset. (Figure adapted from [59], with permission from Elsevier)

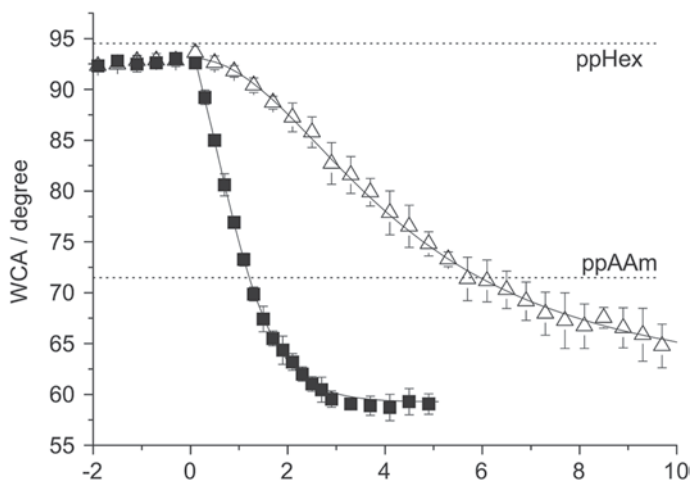


Fig. 5.6 Water contact angle (WCA) along the steep (*square*) and shallow (*triangle*) gradients averaged over 15 measurements. The WCA decreases when going from ppHex (*left*) to ppAAm (*right*). The masked area starts at 0 mm and proceeds to the right of the graph (*positive values*). In the gradient zone the data was fitted with a sigmoidal curve. Error bars represent the standard deviation between 15 measurements from three gradients. (Figure adapted from [59], with permission from Elsevier)

The range and profile of plasma polymer gradients may be tuned by the proximity of the mask depicted in Fig. 5.6 to the sample surface. The larger the gap through which the monomer gas can diffuse, the shallower and longer the resultant gradient. Zelzer et al. deposited a gradient of plasma polymerised hexane (ppHex) over a uniform film of plasma polymerised allylamine (ppAAm), Fig. 5.7. By varying the spacing between the diffusion mask and the substrate they were able to create both steep and shallow gradients of surface energy, which they used to assess the impact of surface wettability on cell adhesion, spreading, and proliferation. Surface roughness of the plasma polymer film was measured by atomic force microscope (AFM) across the gradient, changing from an root-mean-squared (rms) roughness of 0.37–0.38 nm, reinforcing that changes in cell behaviour were in response to surface wettability rather than any topographical cue.(Fig. 5.7)

5.2.2 Biomolecular Gradients

Density of cell binding ligands and other biomolecules on the surface also play a critical role in cell behaviour, and gradients can be created by various methods. Adsorption of extra cellular matrix (ECM) proteins to a predefined gradient or the direct coupling of ligand binding motifs such as RGD peptides have been demonstrated. The ability to control gradients and density of ligand binding motifs represents a powerful tool in creating ‘artificial’ ECM environments to control cell

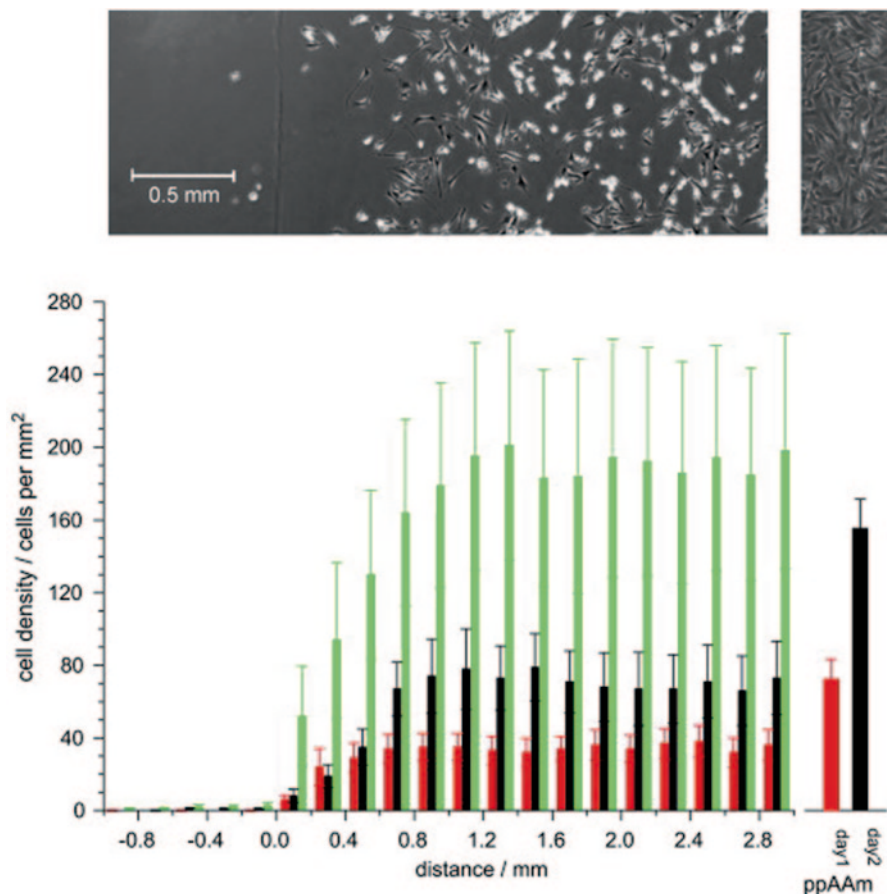
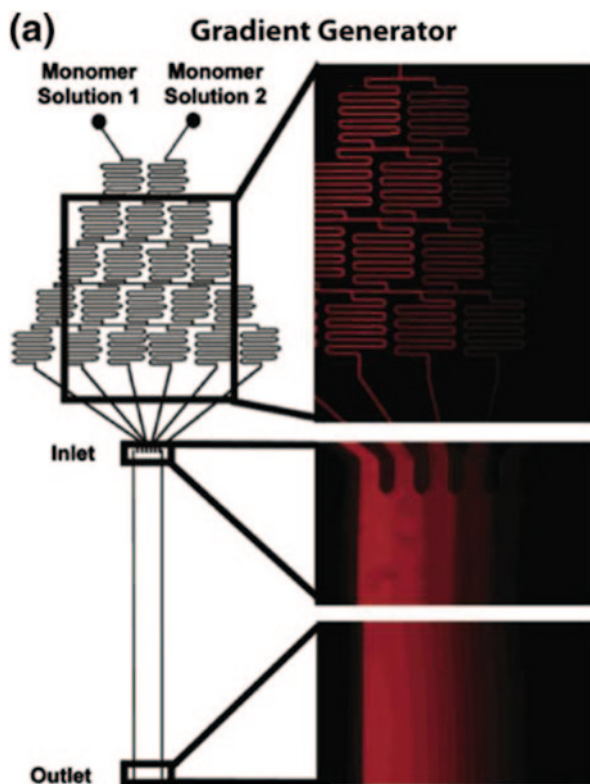


Fig. 5.7 Average cell density across a gradient of wettability. Plasma polymerised allylamine deposited under a diffusion mask has a varied water contact angle over 3 mm. Clear differences in cell morphology can be seen across this gradient in brightfield imaging, *top*. The *lower* figure shows cell response over time, at 1 (*red*), 2 (*black*), and 3 (*green*) days, highlighting the variation in cell density as the hydrophilicity of the surface is continuously varied. (Figure adapted from [59], with permission from Elsevier)

behaviour [42, 79]. Furthermore, microfluidic approaches have also been used to create gradients of common extracellular matrix proteins, for the investigation of cell migration [54, 80; Fig. 5.8].

Both steep and shallow short range chemical gradients may be fabricated by diffusive processes in microfluidic channels, Fig. 5.7, based on the relative concentration of monomer solutions [55]. Parallel channels containing varying concentrations create a stepped gradient at the inlets, which diffuses to form a smooth gradient over a distance of 20 mm. These parallel flows are formed in a gradient generator channel arrangement, which can create a modulated mix of any two input monomer solutions. The gradient profile is dependent of tuning the flow rate of

Fig. 5.8 Chemical gradients can be produced using microfluidic platforms. Hydrogels with a semi continuous variation in composition between two monomers across a channel, adapted from [55], with permission from The American Chemical Society



both monomer solutions—fast monomer flow does not provide sufficient time for a complete diffusion gradient to form, whereas slow monomer flow results in truncating of the gradient range due to excess diffusive mixing. Hydrogel networks with a variation in adhesive ligands (e.g., RGDS) tethered throughout were fabricated by this method. The authors also demonstrated gradients of crosslinking density and hydrogel thickness fabricated through this method. Gradients of adhesive ligands fabricated by this method demonstrated spatial variation of endothelial cell attachment across a 900 μm gradient. Specific ECM protein gradients spanning 500 μm have been created on microstructured substrates [80], whilst similar gradient hydrogels were fabricated by mould casting and photocuring, increasing the gradient dimensions to over 6 cm [81].

Besides surface bound biomolecular gradients, soluble chemical factor gradients have also been created in polymeric microfluidic devices [82]. Mosadegh et al. developed a microfluidic device which generates several chemical gradient conditions on a single platform in flow free microchambers. Polydimethylsiloxane (PDMS) membranes allow the diffusion of chemical gradients whilst protecting cells from shear forces associated with other soluble gradient platforms presented in the literature. There is little or no consideration given to the initial seeding of

cells on gradient platforms by the literature, with this study being a rare exception. Taking care to ensure a homogeneous distribution, either upon seeding cells on a surface gradient, or applying a chemical gradient to the culture environment, is of paramount importance. The majority of experiments conducted on gradients use metrics which depend on uniform initial cell seeding. Cell attachment, chemotaxis, durotaxis, migratory behaviours, and morphological characteristics are all heavily influenced by local cell density. It is possible that uneven initial application of cells may distort results, with certain areas of the gradient appearing to enhance cell attachment and proliferation when in fact they were simply seeded with more cells in the first instance. The use of short range or steep gradients mitigates this risk somewhat, however long range gradients over a few millimetres in length are vulnerable to inhomogeneous cell seeding across the entire gradient area.

5.3 Topographical Gradients

Micro- and nanoscale surface structuring can be used to modify cell behaviour at an interface. Contact guidance, the phenomena in which cells conform to topographical features, can be used to drive cell morphology into a given shape. Polarisation of the cell body, as well as restriction of cell area to a defined size have been extensively demonstrated by differing methods [83]. In order to better understand the impact of geometric cues in cell behaviour, continuous gradient assays are being used to screen cellular response across the full parameter space. The questions raised surrounding the topographical control of cell behaviour have driven the development of new fabrication techniques to create gradients of feature size, pitch, and depth. Etching of plasma polymer films deposited under a diffusion mask [39, 40] and annealing of nanoimprinted gratings on a temperature gradient [51, 84] have been used to create gradients in feature height on a surface and subsequently assess the impact of feature height on cellular contact guidance and migratory behaviours. Greyscale lithography, which varies the intensity of exposure to create varied depth profiles in a photoresist can be used to create topographical gradients, however such methods are sensitive to changes in processing conditions [85]. Direct spatial positioning of a ultraviolet (UV) source provides more reproducible and tuneable control of depth profiles in a photocurable polymer, however this comes at the cost of lateral resolution [86].

5.3.1 *Micro- and Nanopatterned Surfaces*

Fabrication of micro- and nanoscale topographies for biomedical engineering borrows a host of techniques from the semiconductor industry, which has driven increasing resolution in lithographic techniques down to the nanometre over the past decades. This has delivered biomedical engineers a toolbox of surface patterning

techniques, along with some new methods developed specifically to address biological questions. Patterns are generally defined by either direct write (e.g., electron beam lithography (EBL)) or mask based photolithographic approaches. These create topographical features which drive cell behaviour through contact guidance, or spatial distribution of biomolecules or ECM proteins to precisely control cell adhesion to the substrate [22, 26, 87–93].

Micro- and nanogrooves have been shown to direct cellular alignment to a polymeric substrate [24, 94, 95], with various gradient platforms being developed making use of capillary force lithography [18], direct write patterning [15], and plasma polymer deposition [40]. Evidence of cell migration and response to the underlying gradient topography has been demonstrated in the directional migration of fibroblasts along anisotropic grooved substrates [18]. Ultraviolet assisted capillary force lithography was used to create a mould with ridges which were 1 μm in width and 400 nm tall, upon which poly(urethane acrylate) (PUA) films were cast. The spacing between ridges was increased in 100 nm increments across the pattern, creating a linear gradient of pitch. Cell shape and motility was studied at five positions across the gradient, which was relatively steep with average groove width changing from 2.6 to 8.6 μm across a 500 μm pattern, with an absolute variation in groove width across the pattern from 1 to 9.1 μm . These five analysis positions therefore incorporate a substantial range of groove widths into a single datapoint. Cell polarisation and elongation are more pronounced on narrower grooves. Cell migration speeds were optimal at intermediate ridge widths, with cells appearing to migrate towards these intermediate regions from both narrow and wide areas. This indicates that individual cells were capable of sensing and responding to small variations of topographical dimensions underneath them. Sun et al. demonstrated a depth gradient in both groove and ridge polarity, fabricated in polystyrene (PS), polymethylmethacrylate (PMMA), and dimethacrylate (DMA) to separate the effects of surface chemistry and topography on cell alignment [96]. This study found that surface topography had a more prominent impact on cell alignment than surface chemistry for the two materials examined.

Plasma polymerisation has predominantly found use in the creation of chemical coatings and gradients, which may also be functionalized with biomolecules to tune cellular response to a surface. Our group has developed several new applications in micro- and nanofabrication processes, including direct patterning of ppHex films by EBL [97] and use of ppHex as an etch mask for reactive ion etching (RIE) processes [39, 40]. Gradients of plasma polymer thickness, generated by deposition under a diffusion mask (Fig. 5.4c), were deposited across prefabricated etch masks for both nanopillar and microgroove arrays. Upon etching in an RIE process, the variation in film thickness across the etch mask results in a greater etch depth at the thinnest end of the ppHex gradient. Etch rates and material selectivities may be tuned to create a shallow or steep variation in feature height in the prefabricated pattern.(Figs. 5.9, 5.10)

Nanospun fibre meshes represent a bridging between 2D and 3D synthetic environments. Ramalingam et al demonstrated a method of creating a gradient of composition in the final fibre mesh across centimetre length scales [98]. This new technique is applicable to any electrospun polymer, and may be used as either a

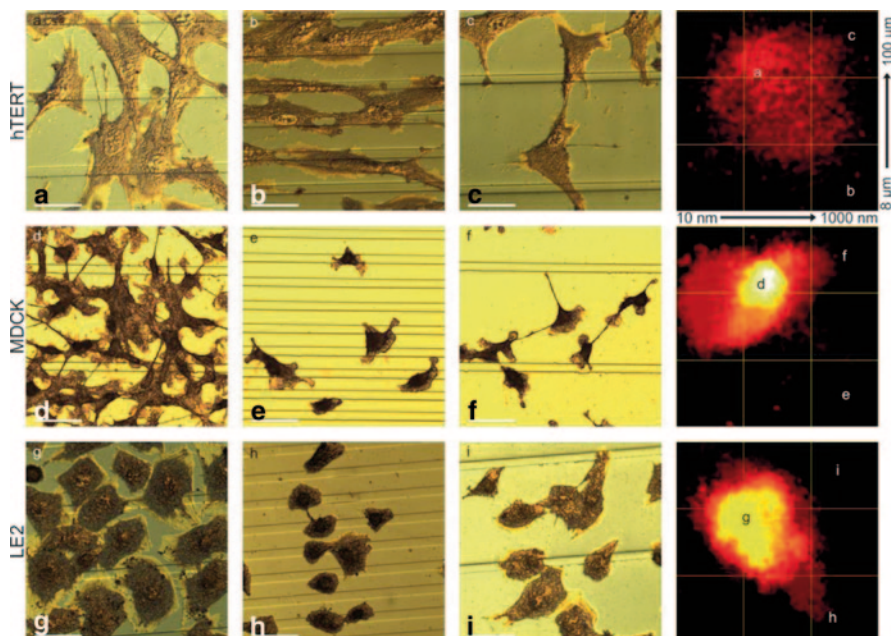


Fig. 5.9 a–i Microscopy images showing clear morphological changes in response to three distinct regions of the dual topography gradient after 72 h, for the three cell types screened. Certain combinations of groove depth and pitch elicit a cell specific response in the fibroblast type hTERT cells when compared to the response of the endothelial (LE2) and epithelial (MDCK) cells. Pseudo-coloured heat maps show the cell coverage over the full 10×10 mm topography, constructed by scanning and averaging six Coomassie stained samples. A clear ‘hot spot’ can be seen for the epithelial and endothelial cell types. Scale bar: 50 μm. (Figure adapted from [40], with permission from John Wiley and Sons)

screening tool to determine ideal blend compositions for a given purpose, or to generate tissue engineering scaffolds for interfacial tissues such as cartilage.

Predominantly, gradients have been fabricated for use to investigate a single cell type, protein or nanoparticle behaviour on a single surface—with homogeneous chemical, topographical, and mechanical properties. For example, fibroblast cells adhere and proliferate rapidly on short polymer phase separated nanotopographies, however this effect is reduced as the nanostructure height increases from 13 to 95 nm to the point where the effect of the topography is reversed [99, 100]. These topographical effects on cell behaviour are not one and the same for all cell types, or geometrical arrangements of nanofeatures of the same length scale. Comparison of the behaviour of fibroblast cells with that of endothelial cells on the same nanostructured array showed an opposite response for each cell type [31].

Our group has increased the information gained from a single experiment by culturing two cell types simultaneously on a nanotopographical gradient, so as to assess the interplay and competition between different cell types and the relative impact of a continuous variation of nanopillar height, Fig. 5.7. As nanopillar height

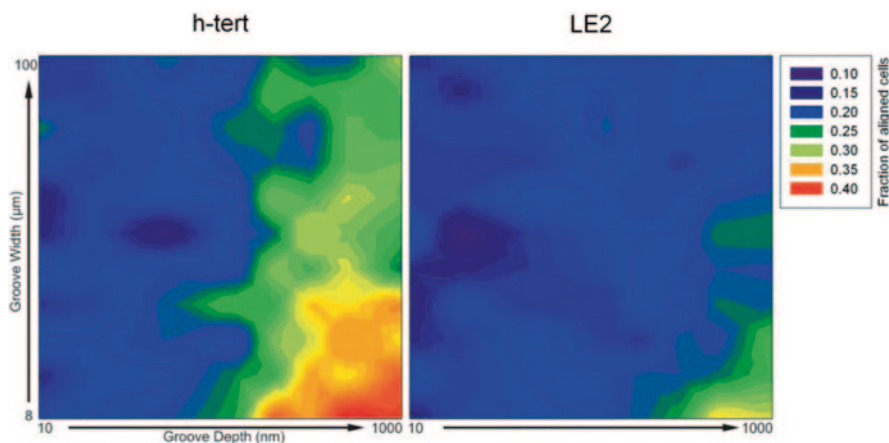


Fig. 5.10 Cellular alignment on the dual gradient topography as a fraction of the total number of cells. **a** hTERT fibroblast type cells exhibit a high degree of alignment to the groove axis where the distance between grooves is lower, and if the grooves are over 500 nm deep. Cells were considered to have aligned to the topography if the major axis of an elliptical fit to their shape lay within $\pm 15^\circ$ of the groove axis. **b** LE2 epithelial type cells show some level of alignment at narrower groove pitches, presumably driven by contact inhibition, however, the higher rate of fibroblast alignment is clear. Sixteen percent of cells on the nonstructured region around the topography fell within this alignment range as expected (30° acceptance over 180°). The groove pitch increases in $0.5 \mu\text{m}$ steps from 8 to $100 \mu\text{m}$, while groove depth increases from under 10 nm to over $1 \mu\text{m}$. (Figure adapted from [40], with permission from John Wiley and Sons)

increases from <10 to 250 nm , the ratio of each cell type in the coculture varies—indicating a cell type specific impact of the nanotopography on cell behaviour. An enrichment of LE2 endothelial cells is evident, whilst hTERT fibroblast cells are simultaneously depleted as the gradient changes from a flat surface to 100 nm tall pillars [39]. A concurrent reduction in total cell number at extreme heights indicates that whilst nanopillar arrays may enrich endothelial populations, there is an upper limit at which their effect becomes detrimental. This reinforces the effectiveness of gradient platforms in optimisation of surfaces which have already been identified as driving the desired biological response. (Fig. 5.11)

5.3.2 Surface Roughness

Whilst sophisticated micro- and nanolithographic techniques have been used to drive cellular behaviour at polymeric surfaces, less precise methods have also been successfully demonstrated as being capable of driving cell behaviour. A continuous gradient of surface roughness in cast epoxy resins revealed higher cell densities on partly roughened surfaces over flat or very rough surfaces—demonstrating the ability of gradient platforms to optimise surface properties [101; Fig. 5.12].

Gradients of surface roughness have also been created in various polymers by applying a temperature gradient across the sample. Poly L lactic acid (PLLA)

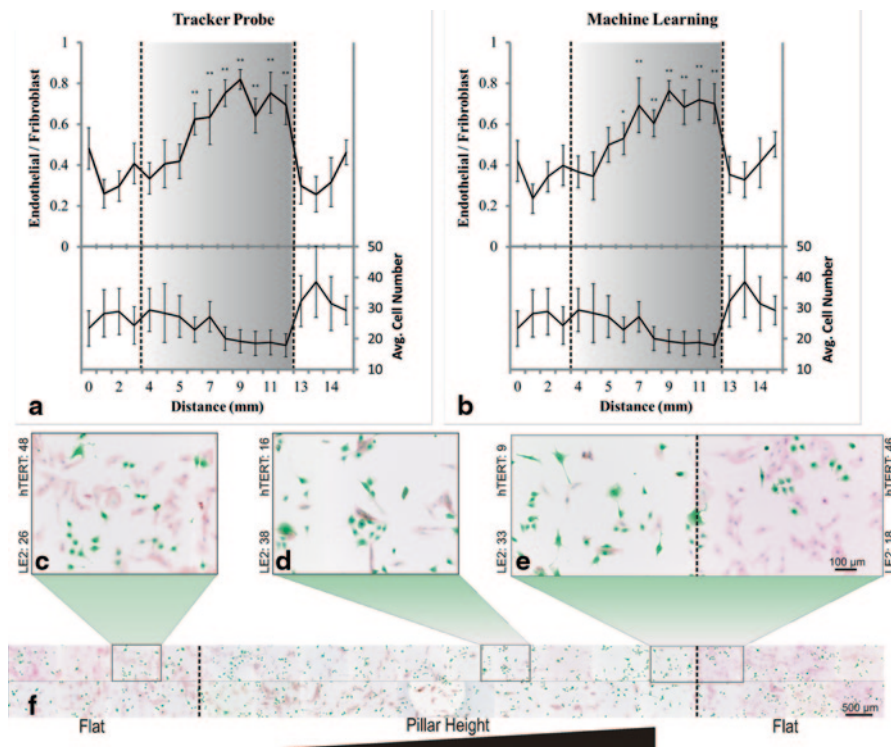


Fig. 5.11 Response of fibroblast (hTERT-BJ1) and endothelial (LE2) cells in coculture to a gradient of nanopillar height is shown. The ratio of endothelial/fibroblast cells after 96 h culture was calculated by **a** direct labelling of the subpopulations with CellTracker probes and **b** applying machine learning to cell morphology and nucleus data to predict cell type; greyscale background gradient represents increasing pillar height from left to right with *dashed line* indicating the nanopillar-flat boundary. Statistically, each datapoint was compared to the ‘baseline’ flat region, $*p < 0.01$, $**p < 0.001$. Images **c–e** show cellular response at various points across the nanogradient sample **f**. From this analysis, we can suggest that a nanopillar height in excess of 75 nm is sufficient to induce a statistically significant change in the ratio of endothelial/fibroblast cells on the nanopattern, however as pillar height increases the average number of cells per frame was found to fall. (Figure adapted from [39], with permission of The American Chemical Society)

crystallinity was continuously varied across a sample by an underlying gradient of annealing temperature [50]. This created a surface roughness gradient with rms roughness values ranging from 0.5 to 13 nm. The total gradient length is not specified, however the method of annealing on a temperature gradient appears to produce a step change in surface roughness rather than a continuously varying gradient, Fig. 5.11c. Alternatively, gradients of surface roughness yielding a gradient of wettability have been achieved by coating a surface in PS polymer nanospheres, then applying a temperature gradient from ambient to above the glass transition temperature of PS [51]. In doing so, the polymer nanospheres experience higher temperatures in one direction, which results in a variation of melting and reflow across the sample. Spheres which are not exposed to any heat remain spherical,

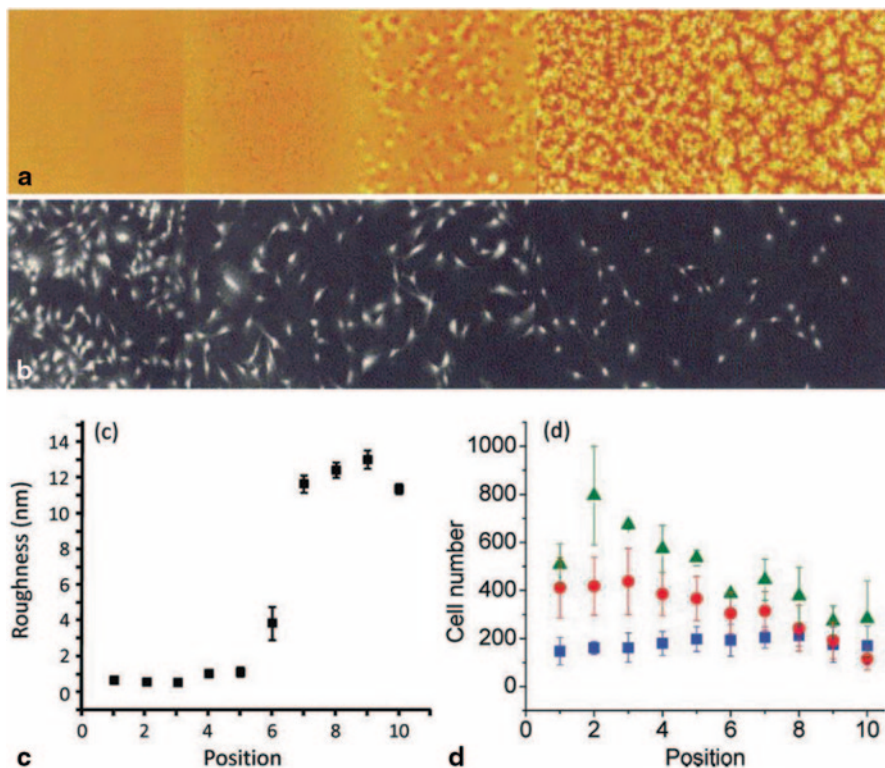


Fig. 5.12 Montage of representative images of PLLA morphology from AFM data (**a** field of view in each image is 20 nm), and corresponding cell count from fluorescent microscopy (**b**, field of view in each image is 1500 nm). Modification of PLLA crystallinity across a millimetre scale by annealing on a temperature gradient yields a continuum of variation in the nanoscale structure of the surface. **a**, MCT3T3-E1 pre-osteoblast cell adhesion was inhibited at increasing levels of roughness. Graph **c** shows average measured roughness as a function of library position. Graph **d** plots average cell number as a function of library position after culturing for 1 (*blue*), 3 (*red*), and 5 (*green*) days. Initial cell attachment is consistent across the gradient substrate, with cell density increasing differentially on areas with lower surface roughness over prolonged culture times. (Figure adapted from [50], with permission from Elsevier)

creating prominent features in the surface. With increasing temperature across the sample, the spheres melt and reflow into less defined structures—creating a long range gradient of surface roughness. Still more control can be achieved: rather than simply annealing polymers on a temperature gradient to create a change in topography, methods utilising stress relaxation in a partially cross linked visco-elastic thin film have been demonstrated [49]. This method employs a combination of soft lithography and differential heating to imprint a uniform structure with nonuniform thermal cross linking of the substrate polymer film. Upon demoulding of the stamp, the temperature dependent stress induced in the film results in a variation in feature amplitude across the pattern.

5.4 Mechanical Gradients

5.4.1 Rigidity Gradients

The mechanical properties of a material signal the stiffness of the local environment to adherent cells, and have been shown to drive differentiation [102], migration [103, 104], and apoptosis [105]. Local variations in stiffness exist within the tissues of the body, and form a key migratory signal for so called durotaxis along a gradient of stiffness [106]. Stiffness of the local environment plays a key role in cell behaviour, and gradients of substrate rigidity have been created in both PDMS and hydrogel materials with stiffness gradients from ‘soft’ to ‘hard’ with compressive moduli ranging from kilopascals to megapascals respectively. This enables studies which span a biologically relevant stiffness gradient, from soft tissues such as the brain with an elastic modulus of approximately 10 kPa, to hard tissues which approach the MPa range such as collagenous bone [102]. Chatterjee et al. showed 3D encapsulation of cells in a poly(ethylene glycol) dimethacrylate (PEGDM) hydrogel with a varied compressive modulus from 10 to 300 kPa, which they achieved through modified monomer concentration across the sample [81]. Osteoblasts cultured within the hydrogel exhibited differentiation lineage commitment which was determined by the stiffness of their local environment—depositing calcified matrix in regions of higher stiffness.

Greyscale lithography was used to create radial gradients of compliance in photocurable polyacrylamide gels. These gradients were relatively shallow, transitioning from a Young’s modulus of 11 kPa in the centre to 2.5 kPa at the edge over a radius of 9 mm [85]. The authors demonstrated that vascular smooth muscle cell motility is influenced by the underlying substrate stiffness, with cells migrating from soft to stiff regions of the substrate and eventually accumulating on stiff regions of the substrate. In fact, cell spreading, polarisation, and motility were all found to increase on gels with uniform stiffness values—whereas cell durotaxis was found to be independent of local stiffness values, and driven by the magnitude of the gradient from soft to stiff [66]. This work demonstrates that minor fluctuations in substrate stiffness can have a drastic impact on cell response, and highlight that any mechanical heterogeneity in supposedly homogeneous surfaces can impact cell behaviour.

Gradients of elasticity are present in physiological contexts such as in muscle, but can also result from pathological conditions. Vincent et al. utilised multiple techniques to generate stiffness gradients in polyacrylamide gels of with shallow and steep rates of change, corresponding to both physiological and pathological states respectively [107, 108]. Steep polymer gradients designed to mimic pathological states had lateral rate of change of between 10 and 40 Pa/ μm , for example a myocardial infarction establishes gradients of approximately 8.5 Pa/ μm [108]. Shallow gradients had a lateral rate of change of approximately 1 Pa/ μm . Step changes in stiffness were also included in the study in the form of 100 μm wide strips of stiff polymer, interspersed with 500 μm wide strips of soft polymer.(Fig. 5.13)

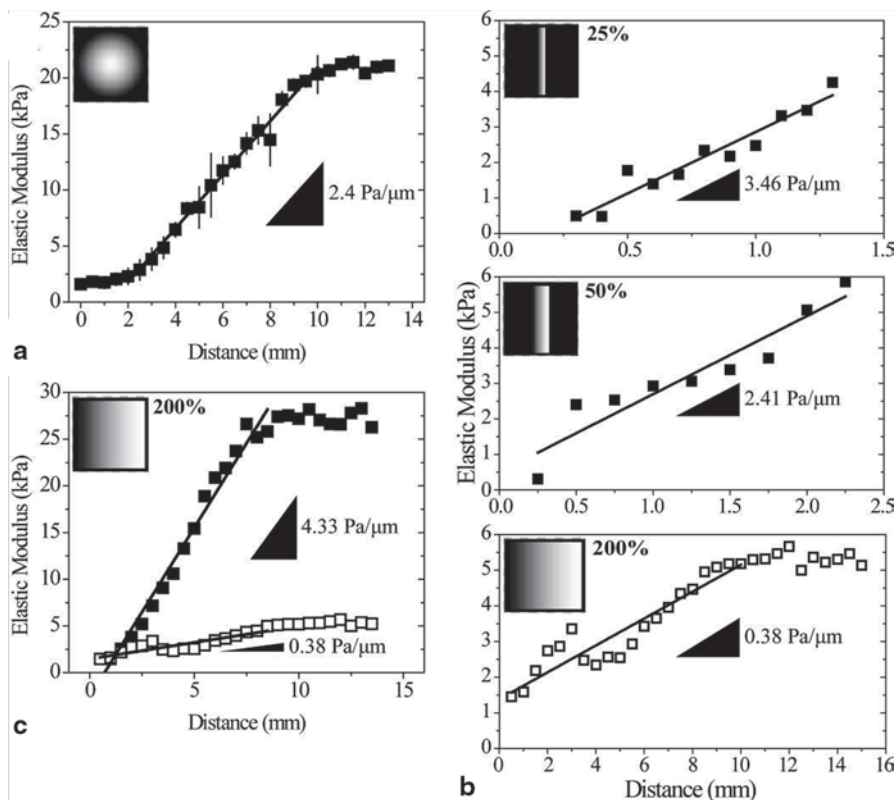


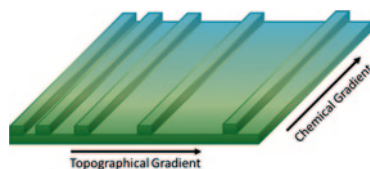
Fig. 5.13 **a** Gradients generated using a radially symmetric mask and a solution containing 10% acrylamide, 0.3% bis-acrylamide, and 0.5% irgacure as the initiator. $n = 4$ gels **b** Gradients produced with the same polymer solution (10% acrylamide, 0.1% bis-acrylamide) but using photomasks where the opacity gradient was scaled to 25%, 50%, or 200% of the distance used in Fig. 5.1 bii, $n = 1$. **c** Two different gradients made with the same photomask but different polymer solutions. Closed squares: 10% acrylamide and 0.3% bis-acrylamide, open squares: 10% acrylamide, 0.1% bis-acrylamide, $n = 1$. Insets **a–c** Photomask images used for gradient fabrication with indicated photomask gradient distance relative to the photomask in Fig. 5.1 bii. (Adapted from [108], reproduced with permission from John Wiley and Sons)

5.5 Combinatorial Gradient Platforms

As cellular response to an engineered surface is complex, and depends on the synergistic effects of multiple properties, creating combined gradients in a single platform can speed up discovery. Combined gradients also allow the relative impact and importance of two distinct surface properties to be investigated at once, as depicted in Fig. 5.3b. Orthogonally positioned gradients of topography and chemistry have been demonstrated in the investigation of multiple surface properties.

Deposition of two allylamine plasma polymer gradients positioned orthogonally, using different polymerisation parameters, were used to create a dual gradient of

Fig. 5.14 A dual gradient of topography and chemistry. Microgroove pitch increases in one direction, whilst wettability increases in the perpendicular direction. (Reproduced from [16], with permission from John Wiley and Sons)



amine functionality on a polypropylene membrane [109]. Wettability was assessed by WCA measurements, showing a range across the sample of $33\text{--}96^\circ$. Fibroblast cells showed extensive elongation and polarisation at a local WCA of $64.5 \pm 9.3^\circ$, with cell proliferation increasing dramatically as the WCA fell to 25.4° . Further to their functionality as wettability gradients, the high density of amine functional groups present in allylamine plasma polymers makes attachment of biomolecules to create more complex gradients possible [110].

Alignment of fibroblast cells to a microgroove substrate with an orthogonally deposited gradient of surface wettability allowed the relative impact of the two distinct cues to be investigated by [16]. Cell coverage and relative alignment to the grooves was analysed after a period of 3 days culture, showing cell alignment to narrow microgrooves was independent of the local WFA.

Dual chemical gradients have been demonstrated in poly(2-hydroxyethyl methacrylate) (PHEMA) which resists the surface adhesion of ECM proteins such as fibronectin [111]. Orthogonal gradients of PHEMA molecular weight and grafting density resulted in a variation of dry thickness across the substrate, and qualitative changes in fibroblast adhesion and morphology (Fig. 5.14)

Gradients of ECM protein concentration have been superimposed over prefabricated topographical structures in PMMA by a microfluidic approach [80]. Comelles et al. report steep fibronectin concentration gradients of $0.5 \text{ pmol} \cdot \text{cm}^{-2} \cdot \text{mm}^{-1}$ which are 40 times higher than previously reported gradients on PMMA substrates [112]. This study used homogeneous topographical patterns, however topographical gradients would also be applicable to this method as used in Fig. 5.15. These gradients of fibronectin molecules, and therefore gradients of adhesive ligand density, effectively control cell adhesion processes—yielding differential cell adhesion and focal contact formation dependent on gradient slope and absolute density.

5.6 Gradient Characterisation

Characterisation of gradients represents a further challenge in effectively applying them to biomedical applications. Many metrology and analysis techniques are currently configured for larger, homogeneous sample areas and are therefore

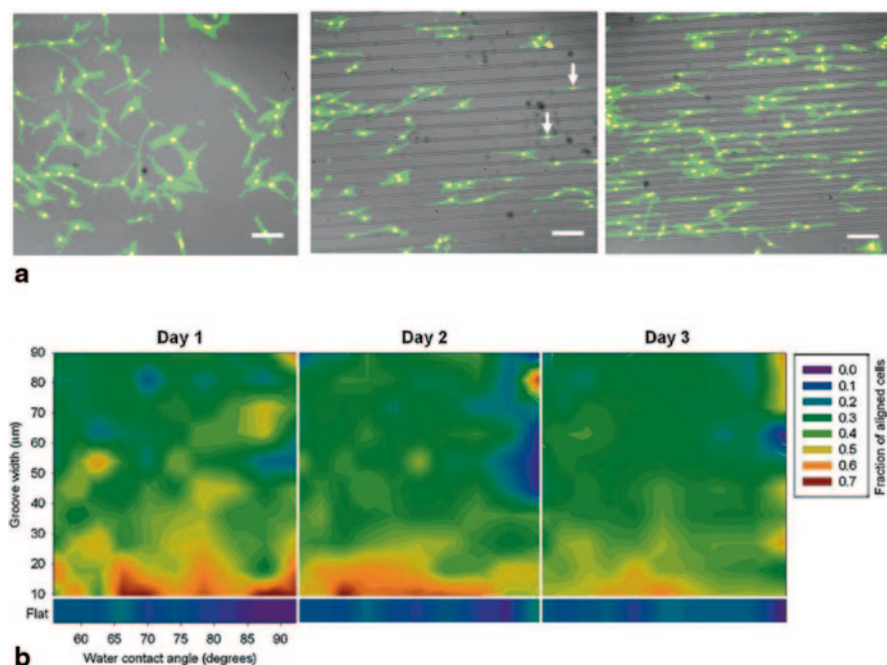


Fig. 5.15 Cell morphology and orientation on orthogonal gradient samples. **a** Typical cell morphology on flat and grooved surfaces at day three. The corresponding WCA range for the three images is approximately between 55° and 58° . Scale bar: $100\ \mu\text{m}$. F-actin fibres in the cytoskeleton were stained using FITC-labelled phalloidin; the nuclei were stained with propidium iodide. **b** Cell alignment on surfaces with orthogonal gradients after 1, 2, and 3 days culture. Cells with an orientation angle less than 10° were defined as aligned, whereas cells with 0° and 90° were classed as being parallel and perpendicular to the groove, respectively. Cell orientations were classified in nine intervals of 10° each, i.e., 0° – 10° , 10° – 20° , etc. For randomly oriented cells, approximately 11% of the whole population was oriented within each one of nine orientation intervals. Data is average of 3 repeats for each image. Each square graph (*grooved area*) and rectangular graph (*flat area*) represents $10 \times 10\ \text{mm}$ and $10 \times 1\ \text{mm}$ areas, respectively. The flat and grooved areas are from the same sample. (Adapted from [16], with permission from John Wiley and Sons)

unsuitable for use in a situation where parameters continuously vary spatially. To that end, picolitre volume WCA analysis, Time-of-Flight Secondary Ion Mass Spectrometry (ToF-SIMS), and optical techniques have been developed to fully characterise gradient surfaces [52]. Mangindaan et al. presented a comprehensive analysis of wettability gradients produced on polypropylene under a diffusion mask in SF_6 plasma [113]. Here, they fabricated a surface with a wide ranging wettability gradient (115° WCA over 10 mm) and fully characterised the plasma-polymer interactions, creating a mathematical model which enables the prediction of wettability based on etch mask design.(Fig. 5.16)

The development of new fabrication methodologies has understandably driven the development of new characterisation methodologies to better determine and quantify the exact properties of these unique surface modifications with sufficient resolution and sensitivity. Analysis of surface energy by measuring the WCA has

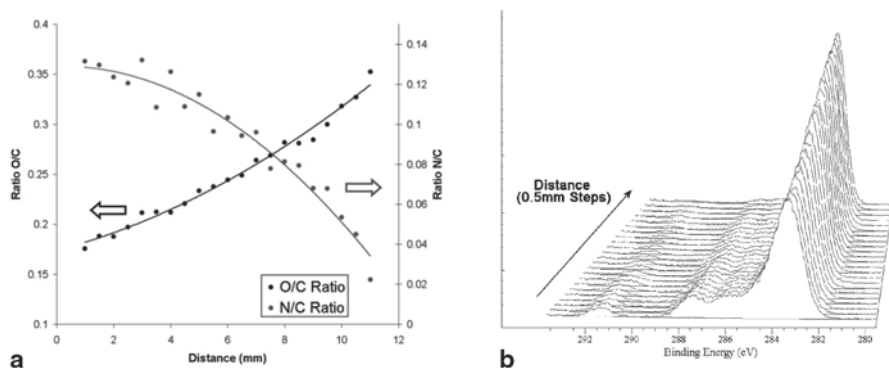


Fig. 5.16 Spatial analysis of chemical gradients by XPS. O/C and N/C ratios as a function of position along an amine-acid chemical gradient, *left*. This shows a changing surface concentration of amine and acid chemistry in opposite directions on the surface. C1s region of a trifluoroethanol derivatised octadiene-acrylic acid chemical gradient, *right*. The reactivity of the surface has been spatially controlled. (Figure adapted from [114], reproduced with permission from The Royal Society of Chemistry)

been refined from microliter volumes on single homogeneous samples through to picolitre volume measurements using automated fluid dispensing and motorised sample stages. This yields millimetre resolution across gradients of surface energy. [59, 70, 84, 115] Chemical composition of the surface may also be analysed using classical techniques such as X-ray photoelectron spectroscopy (XPS) and secondary ion mass spectrometry, where placement and control of the excitation source may be scanned across the gradient surface to yield a readout of its changing properties [114, 116]. Whittle et al. achieved 0.5 mm resolution in XPS analysis of the chemical composition of plasma polymer gradients on glass substrates, including analysis after derivatisation of the deposited chemical groups. Characterisation resolution, in this case, is still limited by the spot size of the XPS tool used, and a continuously varying surface will have inherent differences across a 500 μm analysis region. Cells themselves are often approximately 10–30 μm in size, therefore increased resolution in gradient characterisation is imperative if cell response is to be attributed to a given surface parameter. Other techniques offer increased resolution, such as Fourier transform infrared spectroscopy (FTIR) [117, 118] for chemical gradients or AFM for topographical gradients. Increased resolution, however, increases the burden of acquiring large measurement datasets of slowly changing parameters over a large area.

5.7 Conclusions and Outlook

Gradient platforms represent an effective method of generating a wide range of properties on a single substrate. These allow for the systematic investigation of cellular response to given values or combinations of surface properties. Included in such continuous gradients are more possible values between the initial and final

value, ensuring that the full parameter space is explored, rather than simply one or two possibilities. It is this potential to uncover optimal parameters that has driven the increasing use of gradient platforms in biomaterials research over the past decade. This growing interest has seen the development of over 30 novel techniques for the fabrication of polymeric gradient materials, with new approaches continuing to emerge.

Key to harnessing these powerful and information rich platforms will be similar advances in both characterisation and analysis. As parameters such as surface chemistry are varied continuously over millimetre scale gradients, many surface characterisation techniques cannot capture the fine spatial variation. Techniques such as XPS and WCA measurements have been refined to increase their lateral resolution through motorised stages, smaller spot/drop sizes respectively and automated data acquisition.

Analysis of cell culture experiments on gradient platforms has, however, lagged behind developments of new fabrication and characterisation techniques. We have attempted to take a high content approach, using automated software to screen and characterise cell response based on morphological characteristics [39]. There are significant opportunities to refine the analysis of cell response to gradient substrates beyond simply capturing microscopy data at various points on the gradient. Bringing the full toolset used to interpret cellular response to homogeneous samples across to gradient platforms represents the next step in harnessing the true power of gradient platforms to screen and optimise cellular response.

References

1. Stevens, M. M.; George, J. H. Exploring and Engineering the Cell Surface Interface. *Science* **2005**, *310*, 1135–1138.
2. Geysen, H. M.; Schoenen, F.; Wagner, D.; Wagner, R. Combinatorial Compound Libraries for Drug Discovery: An Ongoing Challenge. *Nat. Rev. Drug Discov.* **2003**, *2*, 222–230.
3. Simon, C. G.; Lin-Gibson, S. Combinatorial and High-Throughput Screening of Biomaterials. *Adv. Mater.* **2011**, *23*, 369–387.
4. Genzer, J.; Bhat, R. R. Surface-Bound Soft Matter Gradients. *Langmuir* **2008**, *24*, 2294–2317.
5. Hook, A. L.; Anderson, D. G.; Langer, R.; Williams, P.; Davies, M. C.; Alexander, M. R. High Throughput Methods Applied in Biomaterial Development and Discovery. *Biomaterials* **2010**, *31*, 187–198.
6. Ankam, S.; Teo, B. K. K.; Kukumberg, M.; Yim, E. K. F. High Throughput Screening to Investigate the Interaction of Stem Cells with Their Extracellular Microenvironment. *Organogenesis* **2013**, *9*, 128–142.
7. Morgenthaler, S.; Zink, C.; Spencer, N. D. Surface-Chemical and -Morphological Gradients. *Soft Matter* **2008**, *4*, 419.
8. Singh, M.; Berkland, C.; Detamore, M. S. Strategies and Applications for Incorporating Physical and Chemical Signal Gradients in Tissue Engineering. *Tissue Eng. Part B* **2008**, *14*.
9. Suk, M.; Khang, G.; Bang, H. Gradient Polymer Surfaces for Biomedical Applications. *Prog. Polym. Sci.* **2008**, *33*, 138–164.
10. Edalat, F. E.; Bae, H.; Manoucheri, S.; Min Cha, J.; Khademhosseini, A. Engineering Approaches Toward Deconstructing and Controlling the Stem Cell Environment. *Ann. Biomed. Eng.* **2012**, *40*, 1301–1315.

11. Voldman, J.; Gray, M. L.; Schmidt, M. a. Microfabrication in Biology and Medicine. *Annu. Rev. Biomed. Eng.* **1999**, *1*, 401–425.
12. Weibel, D. B.; Diluzio, W. R.; Whitesides, G. M. Microfabrication Meets Microbiology. *Nat. Rev. Microbiol.* **2007**, *5*, 209–218.
13. Wu, J.; Mao, Z.; Tan, H.; Han, L.; Ren, T.; Gao, C. Gradient Biomaterials and Their Influences on Cell Migration. *Interface Focus* **2012**, *2*, 337–355.
14. Altomare, L.; Gadegaard, N.; Visai, L.; Tanzi, M. C.; Farè, S. Biodegradable Microgrooved Polymeric Surfaces Obtained by Photolithography for Skeletal Muscle Cell Orientation and Myotube Development. *Acta Biomater.* **2010**, *6*, 1948–1957.
15. Kim, D.-H.; Seo, C.-H.; Han, K.; Kwon, K. W.; Levchenko, A.; Suh, K.-Y. Guided Cell Migration on Microtextured Substrates with Variable Local Density and Anisotropy. *Adv. Funct. Mater.* **2009**, *19*, 1579–1586.
16. Yang, J.; Rose, F. R. a. J.; Gadegaard, N.; Alexander, M. R. A High-Throughput Assay of Cell-Surface Interactions Using Topographical and Chemical Gradients. *Adv. Mater.* **2009**, *21*, 300–304.
17. Kolind, K.; Dolatshahi-Pirouz, A.; Lovmand, J.; Pedersen, F. S.; Foss, M.; Besenbacher, F. A Combinatorial Screening of Human Fibroblast Responses on Micro-Structured Surfaces. *Biomaterials* **2010**, *31*, 9182–9191.
18. Kim, D.-H.; Han, K.; Gupta, K.; Kwon, K. W.; Suh, K.-Y.; Levchenko, A. Mechanosensitivity of Fibroblast Cell Shape and Movement to Anisotropic Substratum Topography Gradients. *Biomaterials* **2009**, *30*, 5433–5444.
19. Lam, M. T.; Sim, S.; Zhu, X.; Takayama, S. The Effect of Continuous Wavy Micropatterns on Silicone Substrates on the Alignment of Skeletal Muscle Myoblasts and Myotubes. *Biomaterials* **2006**, *27*, 4340–4347.
20. Dalby, M. J.; Riehle, M. O.; Yarwood, S. J.; Wilkinson, C. D.; Curtis, A. S. G. Nucleus Alignment and Cell Signaling in Fibroblasts: Response to a Micro-Grooved Topography. *Exp. Cell Res.* **2003**, *284*, 272–280.
21. Meyle, J.; Wolburg, H.; Von Recum, a. F. Surface Micromorphology and Cellular Interactions. *J. Biomater. Appl.* **1993**, *7*, 362–374.
22. Teixeira, A. I.; Abrams, G. a; Bertics, P. J.; Murphy, C. J.; Nealey, P. F. Epithelial Contact Guidance on Well-Defined Micro- and Nanostructured Substrates. *J. Cell Sci.* **2003**, *116*, 1881–1892.
23. Lensen, M. C.; Schulte, V. a.; Salber, J.; Diez, M.; Menges, F.; Möller, M. Cellular Responses to Novel, Micropatterned Biomaterials. *Pure Appl. Chem.* **2008**, *80*, 2479–2487.
24. Miller, C.; Jęftinija, S.; Mallapragada, S. Micropatterned Schwann Cell-Seeded Biodegradable Polymer Substrates Significantly Enhance Neurite Alignment and Outgrowth. *Tissue Eng.* **2001**, *7*, 705–715.
25. Wójciak-Stothard, B.; Curtis, A. S. G.; Monaghan, W.; McGrath, M.; Sommer, I.; Wilkinson, C. D. Role of the Cytoskeleton in the Reaction of Fibroblasts to Multiple Grooved Substrata. *Cell Motil. Cytoskeleton* **1995**, *31*, 147–158.
26. Clark, P.; Connolly, P.; Curtis, A. S. G.; Dow, J. a; Wilkinson, C. D. Topographical Control of Cell Behaviour. I. Simple Step Cues. *Development* **1987**, *99*, 439–448.
27. Wójciak-Stothard, B.; Curtis, A. S. G.; Monaghan, W.; MacDonald, K.; Wilkinson, C. Guidance and Activation of Murine Macrophages by Nanometric Scale Topography. *Exp. Cell Res.* **1996**, *223*, 426–435.
28. Clark, P.; Connolly, P.; Curtis, A. S. G.; Dow, J. a; Wilkinson, C. D. Cell Guidance by Ultrafine Topography in Vitro. *J. Cell Sci.* **1991**, *99 (Pt 1)*, 73–77.
29. Huang, N. F.; Patel, S.; Thakar, R. G.; Wu, J.; Hsiao, B. S.; Chu, B.; Lee, R. J.; Li, S. Myotube Assembly on Nanofibrous and Micropatterned Polymers. *Nano Lett.* **2006**, *6*, 537–542.
30. Dalby, M. J.; Gadegaard, N.; Tare, R.; Andar, A.; Riehle, M. O.; Herzyk, P.; Wilkinson, C. D. W.; Oreffo, R. O. C. The Control of Human Mesenchymal Cell Differentiation Using Nanoscale Symmetry and Disorder. *Nat. Mater.* **2007**, *6*, 997–1003.
31. Csaderova, L.; Martinez, E.; Seunarine, K.; Gadegaard, N.; Wilkinson, C. D. W.; Riehle, M. O. A Biodegradable and Biocompatible Regular Nanopattern for Large-Scale Selective Cell Growth. *Small* **2010**, *6*, 2755–2761.

32. Yim, E. K. F.; Darling, E. M.; Kulangara, K.; Guilak, F.; Leong, W. Nanotopography-Induced Changes in Focal Adhesions, Cytoskeletal Organization, and Mechanical Properties of Human Mesenchymal Stem Cells. *Biomaterials* **2011**, *31*, 1–16.
33. McMurray, R. J.; Gadegaard, N.; Tsimbouri, P. M.; Burgess, K. V.; Mcnamara, L. E.; Tare, R.; Murawski, K.; Kingham, E.; Oreffo, R. O. C.; Dalby, M. J. Nanoscale Surfaces for the Long-Term Maintenance of Mesenchymal Stem Cell Phenotype and Multipotency. *Nat. Mater.* **2011**, 1–8.
34. Yim, E. K. F.; Reano, R. M.; Pang, S. W.; Yee, A. F.; Chen, C. S.; Leong, K. W. Nanopattern-Induced Changes in Morphology and Motility of Smooth Muscle Cells. *Biomaterials* **2005**, *26*, 5405–5413.
35. Yim, E. K. F.; Pang, S. W.; Leong, K. W. Synthetic Nanostructures Inducing Differentiation of Human Mesenchymal Stem Cells into Neuronal Lineage. *Exp. Cell Res.* **2007**, *313*, 1820–1829.
36. Gerecht, S.; Bettinger, C. J.; Zhang, Z.; Borenstein, J. T.; Vunjak-Novakovic, G.; Langer, R. The Effect of Actin Disrupting Agents on Contact Guidance of Human Embryonic Stem Cells. *Biomaterials* **2007**, *28*, 4068–4077.
37. Rebollar, E.; Frischauf, I.; Olbrich, M.; Peterbauer, T.; Hering, S.; Preiner, J.; Hinterdorfer, P.; Romanin, C.; Heitz, J. Proliferation of Aligned Mammalian Cells on Laser-Nanostructured Polystyrene. *Biomaterials* **2008**, *29*, 1796–1806.
38. Tzvetkova-Chevolleau, T.; Stéphaneou, A.; Fuard, D.; Ohayon, J.; Schiavone, P.; Tracqui, P. The Motility of Normal and Cancer Cells in Response to the Combined Influence of the Substrate Rigidity and Anisotropic Microstructure. *Biomaterials* **2008**, *29*, 1541–1551.
39. Reynolds, P.; Pedersen, R. H.; Stormonth-Darling, J.; Dalby, M. J.; Riehle, M. O.; Gadegaard, N. Label-Free Segmentation of Co-Cultured Cells on a Nanotopographical Gradient. *Nano Lett.* **2013**, *13*, 570–576.
40. Reynolds, P. M.; Pedersen, R. H.; Riehle, M. O.; Gadegaard, N. A Dual Gradient Assay for the Parametric Analysis of Cell-Surface Interactions. *Small* **2012**, *8*, 2541–2547.
41. Unadkat, H. V.; Hulsman, M.; Cornelissen, K.; Papenburg, B. J.; Truckenmüller, R. K.; Post, G. F.; Uetz, M.; Reinders, M. J. T.; Stamatiadis, D.; van Blitterswijk, C. a; *et al.* An Algorithm-Based Topographical Biomaterials Library to Instruct Cell Fate. *Proc. Natl. Acad. Sci. U. S. A.* **2011**.
42. Gallant, N. D.; Lavery, K. a.; Amis, E. J.; Becker, M. L. Universal Gradient Substrates for “Click” Biofunctionalization. *Adv. Mater.* **2007**, *19*, 965–969.
43. Genzer, J.; Bhat, R. R. Classification of Key Attributes of Soft Material Gradients. In *Soft Matter Gradient Surfaces: Methods and Applications, First Edition*; 2012.
44. Genzer, J. Surface-Bound Gradients for Studies of Soft Materials Behavior. *Annu. Rev. Mater. Res.* **2012**, *42*, 435–468.
45. Alexander, M. R.; Whittle, J. D.; Barton, D.; Short, R. D. Plasma Polymer Chemical Gradients for Evaluation of Surface Reactivity: Epoxide Reaction with Carboxylic Acid Surface Groups. *J. Mater. Chem.* **2004**, *14*, 408.
46. Menzies, D. J.; Cowie, B.; Fong, C.; Forsythe, J. S.; Gengenbach, T. R.; Mclean, K. M.; Puskar, L.; Textor, M.; Thomsen, L.; Tobin, M.; *et al.* One-Step Method for Generating PEG-Like Plasma Polymer Gradients†: Chemical Characterization and Analysis of Protein Interactions. *Langmuir* **2010**, *252*, 13987–13994.
47. Lee, J. H.; Pazk, J. O. I. W.; Lee, H. B. Cell Adhesion and Growth on Polymer Surfaces with Hydroxyl Groups Prepared by Water Vapour Plasma Treatment. **1991**, *12*, 443–448.
48. Seo, H. S.; Ko, Y. M.; Shim, J. W.; Lim, Y. K.; Kook, J.-K.; Cho, D.-L.; Kim, B. H. Characterization of Bioactive RGD Peptide Immobilized onto Poly(acrylic Acid) Thin Films by Plasma Polymerization. *Appl. Surf. Sci.* **2010**, *257*, 596–602.
49. Roy, S.; Bhandaru, N.; Das, R.; Harikrishnan, G.; Mukherjee, R. Thermally Tailored Gradient Topography Surface on Elastomeric Thin Films. *ACS Appl. Mater. Interfaces* **2014**.
50. Washburn, N. R.; Yamada, K. M.; Simon, C. G.; Kennedy, S. B.; Amis, E. J. High-Throughput Investigation of Osteoblast Response to Polymer Crystallinity†: Influence of Nanometer-Scale Roughness on. *Biomaterials* **2004**, *25*, 1215–1224.

51. Zhang, J.; Xue, L.; Han, Y. Fabrication Gradient Surfaces by Changing Polystyrene Microsphere Topography. *Langmuir* **2005**, *5*–8.
52. Bowen, A. M.; Ritchey, J. A.; Moore, J. S.; Nuzzo, R. G. Programmable Chemical Gradient Patterns by Soft Grayscale Lithography. *Small* **2011**, 3350–3362.
53. Almodóvar, J.; Crouzier, T.; Selimović, Š.; Boudou, T.; Khademhosseini, A.; Picart, C. Gradients of Physical and Biochemical Cues on Polyelectrolyte Multilayer Films Generated via Microfluidics. *Lab Chip* **2013**, *13*, 1562–1570.
54. Gunawan, R. C.; Silvestre, J.; Gaskins, H. R.; Kenis, P. J. A.; Leckband, D. E. Cell Migration and Polarity on Microfabricated Gradients of Extracellular Matrix Proteins. *Langmuir* **2006**, *22*, 4250–4258.
55. Burdick, J. A.; Khademhosseini, A.; Langer, R. Fabrication of Gradient Hydrogels Using a Microfluidics/ Photopolymerization Process. *Langmuir* **2004**, *20*, 8–11.
56. Julthongpipit, D.; Fasaloka, M. J.; Zhang, W.; Nguyen, T.; Amis, E. J. Gradient Chemical Topographies: A Reference Substrate for Surface. *Nano Lett.* **2005**, *5*, 1535–1540.
57. Kreppenhof, K.; Li, J.; Segura, R.; Popp, L.; Rossi, M.; Tzvetkova, P.; Luy, B.; Ka, C. J.; Guber, A. E.; Levkin, P. A. Formation of a Polymer Surface with a Gradient of Pore Size Using a Microfluidic Chip. *Langmuir* **2013**, *29*, 3797–3804.
58. Harding, F. J.; Clements, L. R.; Short, R. D.; Thissen, H.; Voelcker, N. H. Assessing Embryonic Stem Cell Response to Surface Chemistry Using Plasma Polymer Gradients. *Acta Biomater.* **2012**, *8*, 1739–1748.
59. Zelzer, M.; Majani, R.; Bradley, J. W.; Rose, F. R. a J.; Davies, M. C.; Alexander, M. R. Investigation of Cell-Surface Interactions Using Chemical Gradients Formed from Plasma Polymers. *Biomaterials* **2008**, *29*, 172–184.
60. Wells, N.; Baxter, M. a; Turnbull, J. E.; Murray, P.; Edgar, D.; Parry, K. L.; Steele, D. a; Short, R. D. The Geometric Control of E14 and R1 Mouse Embryonic Stem Cell Pluripotency by Plasma Polymer Surface Chemical Gradients. *Biomaterials* **2009**, *30*, 1066–1070.
61. Pitt, W. Fabrication of a Continuous Wettability Gradient by Radio Frequency Plasma Discharge. *J. Colloid Interface Sci.* **1989**, *133*, 223–227.
62. Kim, J.; Carbonell, R. G. Deposition of poly[2-(perfluorooctyl)ethyl Acrylate] from Liquid CO₂ High-Pressure Free Meniscus coating—Uniformity and Morphology. *J. Supercrit. Fluids* **2007**, *42*, 129–141.
63. Ueda-yukoshi, T.; Matsuda, T. Cellular Responses on a Wettability Gradient Surface with Continuous Variations in Surface Compositions of Carbonate and Hydroxyl Groups. **1995**, 4135–4140.
64. Xu, C.; Wu, T.; Mei, Y.; Drain, C. M.; Batteas, J. D.; Beers, K. L. Synthesis and Characterization of Tapered Copolymer Brushes via Surface-Initiated Atom Transfer Radical Copolymerization. **2005**, 11136–11140.
65. Kennedy, S. B.; Washburn, N. R.; Simon, C. G.; Amis, E. J. Combinatorial Screen of the Effect of Surface Energy on Fibronectin-Mediated Osteoblast Adhesion, Spreading and Proliferation. *Biomaterials* **2006**, *27*, 3817–3824.
66. Isenberg, B. C.; Dimilla, P. a; Walker, M.; Kim, S.; Wong, J. Y. Vascular Smooth Muscle Cell Durotaxis Depends on Substrate Stiffness Gradient Strength. *Biophys. J.* **2009**, *97*, 1313–1322.
67. Kuo, C.-H. R.; Xian, J.; Brenton, J. D.; Franze, K.; Sivaniah, E. Complex Stiffness Gradient Substrates for Studying Mechanotactic Cell Migration. *Adv. Mater.* **2012**, *24*, 6059–6064.
68. Zelzer, D. I. M. Plasma Polymer Gradients, University of Nottingham, 2009.
69. Parry, K. L.; Shard, A. G.; Short, R. D.; White, R. G.; Whittle, J. D.; Wright, A. ARXPS Characterisation of Plasma Polymerised Surface Chemical Gradients. *Surf. Interface Anal.* **2006**, 1497–1504.
70. Cantini, M.; Sousa, M.; Moratal, D. Non-Monotonic Cell Differentiation Pattern on Extreme Wettability Gradients. *Biomater. Sci.* **2013**, 202–212.
71. Yasuda, H.; Gazicki, M. Biomedical Applications of Plasma Polymerization and Plasma Treatment of Polymer Surfaces. *Biomaterials* **1982**, *3*, 68–77.

72. Yasuda, H.; Hsu, T. Some Aspects of Plasma Polymerization Investigated by Pulsed R.F. Discharge. *J. Polym. Sci. Polym. Chem. Ed.* **1977**, *15*, 81–97.
73. Yasuda, H.; Hirotsu, T. Critical Evaluation of Conditions of Plasma Polymerization. *J. Polym. Sci. Polym. Chem. Ed.* **1978**, *16*, 743–759.
74. Siow, K. S.; Britcher, L.; Kumar, S.; Griesser, H. J. Plasma Methods for the Generation of Chemically Reactive Surfaces for Biomolecule Immobilization and Cell Colonization—A Review. *Plasma Process. Polym.* **2006**, *3*, 392–418.
75. Van Os, M. T. Surface Modification by Plasma Polymerization: Film Deposition, Tailoring of Surface Properties and Biocompatibility, University of Twente.
76. Smith, T.; Kaelble, D. H.; Hamermesh, C. L. Surface Properties of Metals and Plastic Substrates and Properties of Plasma Polymerized Films on These Substrates Are Reported. *Surf. Sci.* **1978**, *76*, 203–231.
77. Friedrich, J.; Kühn, G.; Mix, R.; Unger, W. Formation of Plasma Polymer Layers with Functional Groups of Different Type and Density at Polymer Surfaces and Their Interaction with Al Atoms. *Plasma Process. Polym.* **2004**, *1*, 28–50.
78. Bilek, M. M.; McKenzie, D. R. Plasma Modified Surfaces for Covalent Immobilization of Functional Biomolecules in the Absence of Chemical Linkers: Towards Better Biosensors and a New Generation of Medical Implants. *Biophys. Rev.* **2010**, *2*, 55–65.
79. Luo, W.; Yousaf, M. N. Tissue Morphing Control on Dynamic Gradient Surfaces. *J. Am. Chem. Soc.* **2011**, *133*, 10780–10783.
80. Comelles, J.; Hortiguera, V.; Samitier, J.; Martinez, E. Versatile Gradients of Covalently Bound Proteins on Microstructured Substrates. *Langmuir* **2012**, *28*, 13688–13697.
81. Chatterjee, K.; Young, M. F.; Simon, C. G. Fabricating Gradient Hydrogel Scaffolds for 3D Cell Culture. *Comb Chem High Throughput Screen* **2011**, *14*, 227–236.
82. Mosadegh, B.; Agarwal, M.; Tavara, H.; Bersano-Begey, T.; Torisawa, Y.; Morell, M.; Wyatt, M. J.; O'Shea, K. S.; Barald, K. F.; Takayama, S. Uniform Cell Seeding and Generation of Overlapping Gradient Profiles in a Multiplexed Microchamber Device with Normally-Closed Valves. *Lab Chip* **2010**, *10*, 2959–2964.
83. Curtis, A. S. G.; Wilkinson, C. Topographical Control of Cells. *Biomaterials* **1997**, *18*, 1573–1583.
84. Ashley, K. M.; Meredith, J. C.; Amis, E.; Raghavan, D.; Karim, A. Combinatorial Investigation of Dewetting: Polystyrene Thin Films on Gradient Hydrophilic Surfaces. *Polymer (Guildf)*. **2003**, *44*, 769–772.
85. Wong, J. Y.; Velasco, A.; Rajagopalan, P.; Pham, Q. Directed Movement of Vascular Smooth Muscle Cells on Gradient-Compliant Hydrogels. **2003**, 1908–1913.
86. Berry, B. C.; Stafford, C. M.; Pandya, M.; Lucas, L. a; Karim, A.; Faslka, M. J. Versatile Platform for Creating Gradient Combinatorial Libraries via Modulated Light Exposure. *Rev. Sci. Instrum.* **2007**, *78*, 072202.
87. Nakajima, M.; Ishimuro, T.; Kato, K.; Ko, I.; Hirata, I.; Arima, Y.; Iwata, H. Combinatorial Protein Display for the Cell-Based Screening of Biomaterials That Direct Neural Stem Cell Differentiation. *Biomaterials* **2007**, *28*, 1048–1060.
88. Xu, F.; Wu, J.; Wang, S.; Durmus, N. G.; Gurkan, U. A.; Demirci, U. Microengineering Methods for Cell-Based Microarrays and High-Throughput Drug-Screening Applications. *Biofabrication* **2011**, *3*, 034101.
89. Khademhosseini, A.; Langer, R.; Borenstein, J.; Vacanti, J. P. Microscale Technologies for Tissue Engineering and Biology. *Proc. Natl. Acad. Sci. U. S. A.* **2006**, *103*, 2480–2487.
90. Alom Ruiz, S.; Chen, C. S. Microcontact Printing: A Tool to Pattern. *Soft Matter* **2007**, *3*, 168.
91. Zhou, X.; Hu, J.; Li, J.; Shi, J.; Chen, Y. Patterning of Two-Level Topographic Cues for Observation of Competitive Guidance of Cell Alignment. *ACS Appl. Mater. Interfaces* **2012**, *4*, 3888–3892.
92. Ferrari, A.; Cecchini, M.; Serresi, M.; Faraci, P.; Pisignano, D.; Beltram, F. Neuronal Polarity Selection by Topography-Induced Focal Adhesion Control. *Biomaterials* **2010**, *31*, 4682–4694.

93. Altomare, L.; Riehle, M.; Gadegaard, N.; Tanzi, M. C.; Farè, S. Microcontact Printing of Fibronectin on a Biodegradable Polymeric Surface for Skeletal Muscle Cell Orientation. *Int. J. Artif. Organs* **2010**, *33*, 535–543.
94. Charest, J. L.; García, A. J.; King, W. P. Myoblast Alignment and Differentiation on Cell Culture Substrates with Microscale Topography and Model Chemistries. *Biomaterials* **2007**, *28*, 2202–2210.
95. Fraser, S. a; Ting, Y.-H.; Mallon, K. S.; Wendt, A. E.; Murphy, C. J.; Nealey, P. F. Sub-Micron and Nanoscale Feature Depth Modulates Alignment of Stromal Fibroblasts and Corneal Epithelial Cells in Serum-Rich and Serum-Free Media. *J. Biomed. Mater. Res. Part A* **2008**, *86*, 725–735.
96. Sun, J.; Ding, Y.; Lin, N. J.; Zhou, J.; Ro, H.; Soles, C. L.; Cicerone, M. T.; Lin-gibson, S. Exploring Cellular Contact Guidance Using Gradient Nanogratings. *Biomacromolecules* **2010**, *3067–3072*.
97. Pedersen, R. H.; Hamzah, M.; Thoms, S.; Roach, P.; Alexander, M. R.; Gadegaard, N. Electron Beam Lithography Using Plasma Polymerized Hexane as Resist. *Microelectron. Eng.* **2010**, *87*, 1112–1114.
98. Ramalingam, M.; Young, M. F.; Thomas, V.; Limin, S.; Chow, L. C.; Miles, W. C.; Simon, C. G. Nanofiber Scaffold Gradients for Interfacial Tissue Engineering. *J. Biomater. Appl* **2013**, *27*, 695–705.
99. Dalby, M. J.; Riehle, M. O.; Johnstone, H. J. H.; Affrossman, S.; Curtis, A. S. G. Nonadhesive Nanotopography: Fibroblast Response to Poly(n-Butyl Methacrylate)-Poly(styrene) Demixed Surface Features. *J. Biomed. Mater. Res. A* **2003**, *67*, 1025–1032.
100. Dalby, M. J.; Giannaras, D.; Riehle, M. O.; Gadegaard, N.; Affrossman, S.; Curtis, A. S. G. Rapid Fibroblast Adhesion to 27 nm High Polymer Demixed Nano-Topography. *Biomaterials* **2004**, *25*, 77–83.
101. Kunzler, T. P.; Drobek, T.; Schuler, M.; Spencer, N. D. Systematic Study of Osteoblast and Fibroblast Response to Roughness by Means of Surface-Morphology Gradients. *Biomaterials* **2007**, *28*, 2175–2182.
102. Engler, A. J.; Sen, S.; Sweeney, H. L.; Discher, D. E. Matrix Elasticity Directs Stem Cell Lineage Specification. *Cell* **2006**, *126*, 677–689.
103. Pelham, R. J.; Wang, Y.-L. Cell Locomotion and Focal Adhesions Are Regulated by Substrate Flexibility. *Proc. Natl. Acad. Sci.* **1997**, *94*.
104. Lo, C.; Wang, H.; Dembo, M.; Wang, Y. Cell Movement Is Guided by the Rigidity of the Substrate. *Biophys. J.* **2000**, *79*, 144–152.
105. Fu, J.; Wang, Y.; Yang, M. T.; Desai, R. A.; Yu, X.; Liu, Z.; Chen, C. S. Mechanical Regulation of Cell Function with Geometrically Modulated Elastomeric Substrates. *Nat. Publ. Gr.* **2010**, *7*, 733–736.
106. Seidi, A.; Ramalingam, M.; Elloumi-Hannachi, I.; Ostrovidov, S.; Khademhosseini, A. Gradient Biomaterials for Soft-to-Hard Interface Tissue Engineering. *Acta Biomater.* **2011**, *7*, 1441–1451.
107. Tse, J. R.; Engler, A. J. Stiffness Gradients Mimicking in Vivo Tissue Variation Regulate Mesenchymal Stem Cell Fate. *PLoS One* **2011**, *6*, e15978.
108. Vincent, L. G.; Choi, Y. S.; Alonso-Latorre, B.; Del Álamo, J. C.; Engler, A. J. Mesenchymal Stem Cell Durotaxis Depends on Substrate Stiffness Gradient Strength. *Biotechnol. J.* **2013**, *8*, 472–484.
109. Mangindaan, D.; Kuo, W.; Wang, M. Two-Dimensional Amine-Functionality Gradient by Plasma Polymerization. *Biochem. Eng. J.* **2013**, *78*, 198–204.
110. Basarir, F.; Cuong, N.; Song, W.-K.; Yoon, T.-H. Surface Modification via Plasma Polymerization of Allylamine for Antibody Immobilization. *Macromol. Symp.* **2007**, *249–250*, 61–66.
111. Bhat, B. R. R.; Chaney, B. N.; Rowley, J.; Liebmann-vinson, A.; Genzer, J. Tailoring Cell Adhesion Using Surface-Grafted Polymer Gradient Assemblies. *Adv. Mater.* **2005**, *17*, 2802–2807.

112. Lagunas, A.; Comelles, J.; Marti, E; Samitier, J. Universal Chemical Gradient Platforms Using Poly (Methyl Methacrylate) Based on the Biotin—Streptavidin Interaction for Biological Applications. *Langmuir* **2010**, *26*, 14154–14161.
113. Mangindaan, D.; Kuo, W.; Wang, Y; Wang, M. Experimental and Numerical Modeling of the Controllable Wettability Gradient on Poly (Propylene) Created by SF 6 Plasma. *Plasma Process. Polym.* **2010**, *7*, 754–765.
114. Whittle, J. D.; Barton, D.; Alexander, R.; Short, R. D.; Robert, S.; Building, H.; Street, M; Uk, S. A Method for the Deposition of Controllable Chemical Gradients †. *Chem. Commun. (Camb)*. **2003**, 1766–1767.
115. Zelzer, M.; Alexander, M. R.; Russell, N. A. Acta Biomaterialia Hippocampal Cell Response to Substrates with Surface Chemistry Gradients. *Acta Biomater.* **2011**, *7*, 4120–4130.
116. Menzies, D. J.; Jasieniak, M.; Griesser, H. J.; Forsythe, J. S.; Johnson, G.; Mcfarland, G. A.; Muir, B. W. A ToF-SIMS and XPS Study of Protein Adsorption and Cell Attachment across PEG-like Plasma Polymer Films with Lateral Compositional Gradients. *Surf. Sci.* **2012**, *606*, 1798–1807.
117. Eidelman, N.; Simon, C. G. Blend Composition Gradients by FTIR Microspectroscopy. **2004**, *109*, 219–231.
118. l’Abee, R.; Li, W.; Goossens, H; van Duin, M. Application of FTIR Microscopy in Combinatorial Experimentation on Polymer Blends. *Macromol. Symp.* **2008**, *265*, 281–289.